Electronic Supplementary Material (ESI) for Journal of Materials Chemistry A.

Supplementary Materials for

Approaching the Shockley-Queisser limit for fill factors in lead-tin mixed perovskite photovoltaics

K.D.G.I. Jayawardena,[a†] R.M.I. Bandara,[a†] M. Monti,[b] E. Butler-Caddle,[b] T. Pichler,[c] H. Shiozawa,[c,d] Z. Wang,[e] S. Jenatsch,[f] S.J.Hinder,[g] M.G.Masteghin,[a] M. Patel,[h] H.M. Thirimanne,[a] W. Zhang,[a] R.A. Sporea,[a] J. Lloyd-Hughes,[b] S.R.P. Silva[a]*

Correspondence to: s.silva@surrey.ac.uk

XRD analysis

In the range of the measurement, 4 distinctive peaks are seen (**Fig. S4**) at 2θ values of ~14^0, ~20^0, ~24^0 and ~28^0 which were identified to be corresponding to 100, 110, 111, 200 planes respectively, as seen in prior reports for triple cation perovskites.[1] The occurrence of an excess PbI_2 phase is not seen in the LTM films as can be seen by the lack of any peaks at lower 2θ values near the main 100 perovskite peak. The peak positions have shifted to higher 2θ values following the GABr treatment. When fitted with the orthorhombic model;

$$\frac{1}{d_{hkl}^2} = \frac{h^2}{a^2} + \frac{k^2}{b^2} + \frac{l^2}{c^2} \quad \text{(S1)}$$

the unit cell parameters can be calculated as, a = 6.33 Å, b = 6.34 Å, c = 6.34 Å for the reference LTM and a = 6.32 Å, b = 6.29 Å and c = 6.33 Å for the GABr treated LTM, clearly showing the contraction of unit cells following the GABr treatment.

Modified Williamson-Hall method for microstrain estimation

Reduction in grain size (Scherrer broadening) and/or non-uniform strain (microstrain) causes a broadening and peak shifts in XRD spectra. It is noted that Scherrer broadening is significant only for grains whose sizes are less than 100 nm which is below that, observed in this work. For crystalline materials, small fluctuations in the lattice spacing as a result of crystal imperfections/structural defects including dislocations, vacancies, stacking faults, interstitials, twinning and grain boundaries[2–4] can result in microstrain. By considering Braggs law[5]:

$$n\lambda = 2dsin\theta \quad \text{(S2)}$$

where n is an integer, λ is the wavelength of the X-ray energy used, d represents the lattice parameter and θ represents the diffraction angle, it is evident that small fluctuations in d results in small fluctuations, or broadening, in θ. For this work, the extent of microstrain in the LTM perovskite films studied in this work were evaluated by analyzing the peak broadening in the diffraction patterns based on the modified Williamson-Hall method[2,4]. Under experimental conditions, three factors affect the effective d-space broadening (Δd_{obs}) of an XRD peak. This includes the instrument response (Δd_{ins}), the grain size (Δd_{size}) and the microstrain (Δd_{ε}) width

broadening, which contributes towards the Gaussian full width half maximum broadening in the 2θ scan. These can be de-convoluted from the observed broadening, via,

$$\Delta d_{obs}^{2} = \Delta d_{\varepsilon}^{2} + \Delta d_{ins}^{2} + \Delta d_{\varepsilon ize}^{2} \quad \text{(S3)}$$

In the above, the unit-less microstrain ε is defined as $\varepsilon = (d_{\varepsilon}/d)$, where d is the mean d-spacing. As mentioned above, based on the grain sizes observed in this work, the size effect induced peak width broadening can be neglected. Therefore,

$$\left(\Delta_{obs}^{2} - \Delta_{ins}^{2}\right)^{1/2} \approx \varepsilon d \quad \text{(S4)}$$

As a result, the microstrain, ε, in the crystals can be estimated from the slope of $\left(\Delta_{obs}^{2} - \Delta_{ins}^{2}\right)^{1/2}$ vs d. In contrast to the pristine perovskite film, we can clearly observe an increase in microstrain following the GABr treatment which is attributed to the formation of $Cs_{0.05}FA_{0.79}MA_{0.16}Pb_{0.5}Sn_{0.5}(I_{0.8}Br_{0.2})_3$ perovskite phase at the grain boundaries of $Cs_{0.05}FA_{0.79}MA_{0.16}Pb_{0.5}Sn_{0.5}I_3$ and on the film surface.

Estimation of bandgap energies

To estimate the bandgap energies of the LTM films, the steady state photoluminescence (PL) spectra of the two films were investigated. Each film was excited at 475 nm from both surfaces as shown in **Fig. S5**. The resulting spectra show a blue-shift in the peak positions following the GABr treatment. In order to determine the bandgap energies of the LTM perovskites, the back excited PL spectra were fitted with Voigt functions, and centre x-values are taken as the E_{BG}.

Estimation of work function

The work functions were measured with He Iα (21.22 eV) on the sample biased at -5 V and the valence band spectra were measured at room temperature with He II (40.8 eV).

The work function (Φ_S) was evaluated as:

$$\Phi_S = E_{cutoff} + E_{bias} + \Phi_A \quad \text{(S8)}$$

where E_{cutoff} is the low-kinetic energy cutoff (evaluated in **Fig. 7a** & **b**); Reference 5.243 eV and GABr 5.163 eV), E_{bias} is the bias potential (-5V) and Φ_A is the work function of the analyser (4.135 eV).

Φ_A was evaluated from the Fermi level of Au(111) single crystal. The work functions with respect to the vaccum level (fermi level; E_f)were calculated as -4.4 eV for the reference LTM and -4.3 eV for the GABr treated LTM.

The valence level with respect to the work function was calculated by the onset of the valence band in each sample (**Fig. 7c**). There appears to be an energy offset of the two samples where the GABr treatment has shifted onset to 1.037 eV compared to 0.827 eV for the reference. The valence band positions were hence calculated to be -5.2 eV for the reference sample and -5.3 eV for GABr LTM. The conduction band positions were evaluated by:

$$CB = VB - E_{BG} \quad \text{(S9)}$$

where, CB and VB denotes conduction and valence band energies and E_{BG} is the bandgap energy. As calculated conduction band energies are -3.9 eV for reference and -4.0 eV for GABr LTM.

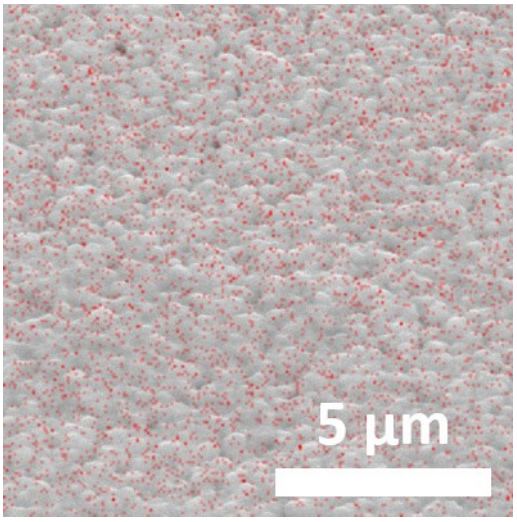

Fig. S1. The EDX mapping of surface of the treated perovskite layer showing homogeneous Br^- distribution (indicated by red dots) laid on top of the SEM micrograph of the tested LTM perovskite surface.

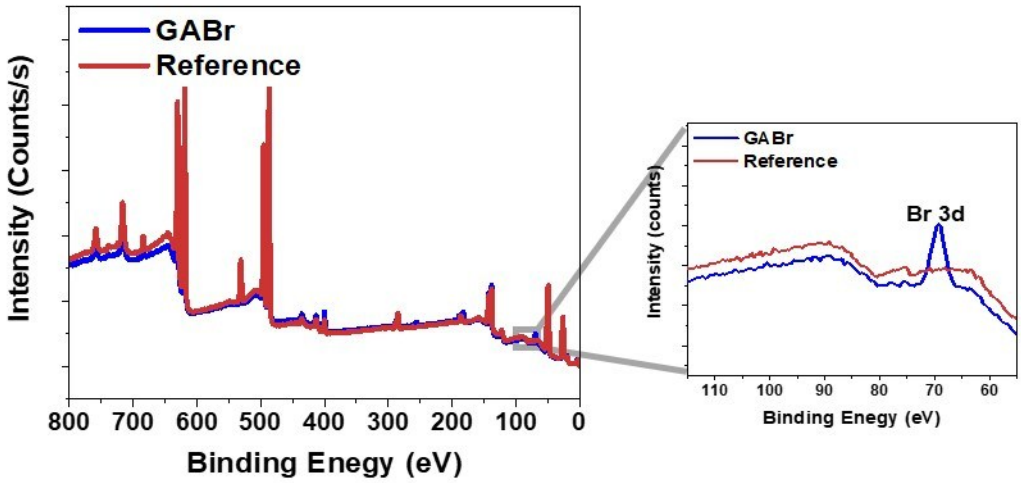

Fig. S2. XPS surface analysis of LTM thin films. The Br 3d peak is clearly visible for the GABr treated sample whereas the reference does not show any such feature. Here, the Br(3d) and I($3d^5$) atomic percentages are 4.37% and 17.07%, resulting in a Br^{-1}: I^{-1} ration of 0.2:0.8. The rest of the spectra are largely seen to be similar in both LTM films showing no major changes in the elemental structure due to the surface treatment.

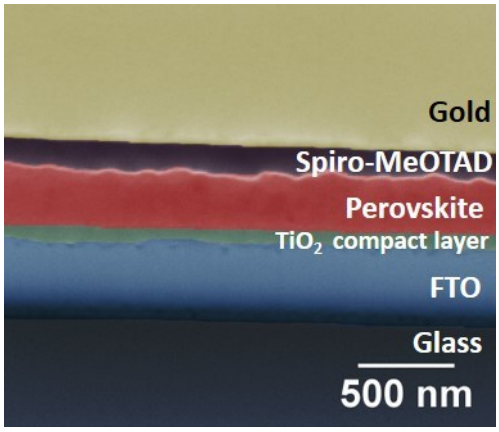

Fig. S3. Cross sectional SEM image of a $Cs_{0.05}FA_{0.79}MA_{0.16}Pb(I_{0.85}Br_{0.15})_3$ film. A bright capping layer on the perovskite layer is observed despite the lack of any additional surface passivation.

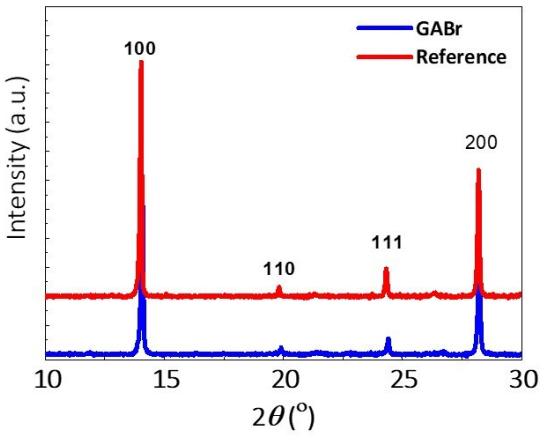

Fig. S4. XRD spectra of LTM perovskite films. Shift in peaks are seen following the GABr treatment to lower lattice spacing.

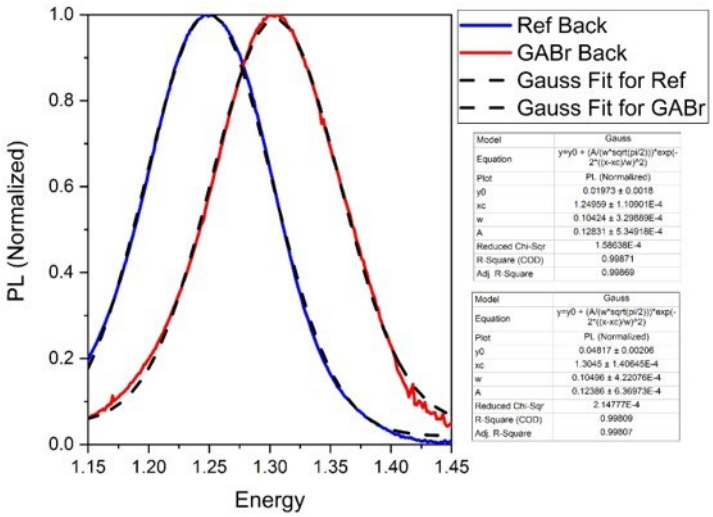

Fig. S5. Fits for determination of bandgap energy (E_{BG}) based on steady state PL spectra obtained from back excitation of the perovskite layer (excitation wavelength = 475 nm). The spectra are fitted with Voigt functions (fittings shown in dotted lines) to obtain the bandgap.

References

1 H. Tsai, R. Asadpour, J.-C. Blancon, C.C. Stoumpos, O. Durand, J.W. Strzalka, B. Chen, R. Verduzco, P.M. Ajayan, S. Tretiak, J. Even, M.A. Alam, M.G. Kanatzidis, W. Nie and A.D. Mohite, *Science,* 2018, **360**, 67–70.

2 I. Robinson and R. Harder, *Nat. Mater*. 2009, **8**, 291–298.

3 A. Pramanick, X.P. Wang, C. Hoffmann, S.O. Diallo, M.R. V. Jørgensen and X.-L. Wang, *Phys. Rev. B*., 2015, **92**, 174103.

4 G. Williamson and W. Hall, *Acta Metall*. 1953, **1**, 22–31.

5 M. Birkholz, P.F. Fewster and C. Genzel, *Thin film analysis by X-ray scattering*, Wiley-VCH, 2006.